Clinical Kidney Journal, 2021, vol. 14, no. 10, 2420–2427

doi: 10.1093/ckj/sfab088
Advance Access Publication Date: 1 May 2021
Original Article

ORIGINAL ARTICLE

Functional megalin is expressed in renal cysts in a mouse model of adult polycystic kidney disease

Marlene L. Nielsen [1,*], Mia C. Mundt[1,*], Dorte L. Lildballe[2], Maria Rasmussen [3,4], Lone Sunde [1,5], Vicente E. Torres[6,7], Peter C. Harris[6,7] and Henrik Birn[1,8]

[1]Department of Biomedicine, Aarhus University, Aarhus C, Denmark, [2]Department of Molecular Medine, Aarhus University Hospital, Aarhus N, Denmark, [3]Department of Clinical Genetics, Lillebaelt Hospital, University Hospital of Southern Denmark, Vejle, Denmark, [4]Department of Regional Health Research, University of Southern Denmark, Odense C, Denmark, [5]Department of Clinical Genetics, Aalborg University Hospital, Aalborg C, Denmark, [6]Department of Nephrology and Hypertension, Mayo Clinic, Rochester, MN, USA, [7]Department of Internal Medicine, Mayo Clinic, Rochester, MN, USA and [8]Department of Renal Medicine, Aarhus University Hospital, Aarhus N, Denmark

Correspondence to: Marlene L. Nielsen; E-mail: marlene.n@biomed.au.dk
*These authors contributed equally to this work.

ABSTRACT

Background. Autosomal dominant polycystic kidney disease (ADPKD) is characterized by the progressive growth of cysts and a decline of renal function. The clinical feasibility of the number of potential disease-modifying drugs is limited by systemic adverse effects. We hypothesize that megalin, a multiligand endocytic receptor expressed in the proximal tubule, may be used to facilitate drug uptake into cysts, thereby allowing for greater efficacy and fewer side effects.

Methods. The cyst expression of various tubular markers, including megalin and aquaporin 2 (AQP2), was analysed by immunohistochemistry (IHC) of kidney sections from the ADPKD mouse model ($PKD1^{RC/RC}$) at different post-natal ages. The endocytic function of megalin in cysts was examined by IHC of kidney tissue from mice injected with the megalin ligand aprotinin.

Results. Cyst lining epithelial cells expressing megalin were observed at all ages; however, the proportion decreased with age. Concomitantly, an increasing proportion of cysts revealed expression of AQP2, partial expression of megalin and/or AQP2 or no expression of the examined markers. Endocytic uptake of aprotinin was evident in megalin-positive cysts, but only in those that remained connected to the renal tubular system.

Conclusions. Megalin-expressing cysts were observed at all ages, but the proportion decreased with age, possibly due to a switch in tubular origin, a merging of cysts of different tubular origin and/or a change in the expression pattern of cyst lining cells. Megalin expressed in cysts was functional, suggesting that megalin-mediated endocytosis is a potential mechanism for drug targeting in ADPKD if initiated early in the disease.

Received: 18.12.2020; Editorial decision: 6.4.2021

Keywords: ADPKD, cystogenesis, immunohistochemistry, proximal tubule, targeted treatment

INTRODUCTION

Autosomal dominant polycystic kidney disease (ADPKD) is the most common inherited kidney disorder, with a reported prevalence of 1/1000–1/2000 in the general population [1, 2]. ADPKD is genetically heterogeneous and is mainly associated with pathogenic variants in two genes, *PKD1* and *PKD2*, which encode the membrane proteins polycystin 1 (PC1) and polycystin 2 (PC2), respectively [3, 4]. The disease is characterized by progressive growth of kidney cysts, causing a decline in renal function and leading to end-stage renal disease (ESRD) [5] in ~50% of patients by the sixth decade of their life [6, 7]. While present-day interventions may slow disease progression, there is currently no available treatment that efficiently blocks the progression of cyst formation and growth, in part because the dosing is limited by systemic adverse effects resulting from targeting of other organs [8]. Multiple studies in rodent models of ADPKD have shown that in the early stage of disease, cyst formation mainly initiates from the proximal tubules (PTs), after which a tubular switch in cyst origin is observed [9–11]. In the kidney, megalin is selectively expressed within the brush border located at the apical membrane of PT cells, where it serves as a multiligand receptor essential to reabsorption of a large number of filtered substances, including drugs [12]. Megalin has previously been explored as a kidney-specific drug-targeting receptor in which the conjugate was efficiently endocytosed and accumulated exclusively in the PT cells [13]. Based on these findings, we hypothesized that megalin may be used to facilitate drug uptake in megalin-expressing cyst lining epithelial cells (referred to as cystic cells hereafter), thereby increasing efficacy and reducing adverse effects. To substantiate the applicability of this approach, we examined the temporal expression and function of megalin in cystic kidney tissue from a $PKD1^{RC/RC}$ mouse model of ADPKD.

MATERIALS AND METHODS

Ethics statement

Animals used in all experiments were maintained and subjected to procedures according to the guidelines and approval of the Danish Animal Experiment Inspectorate (2019-15-0201-01631).

Animal model

The ADPKD mouse model $PKD1^{RC/RC}$ has previously been published [9]. The mice were housed in a 12-h day/night cycle, a temperature of 21°C and bred homozygous in the animal facility at the Department of Biomedicine, Aarhus University. Ten mice (five of each sex) were anaesthetized by isoflurane inhalation at post-natal (P) age 10, 20, 30, 90 and 180 days and, when possible, kidneys were perfusion fixed through the aorta (or otherwise immersion fixed) with 2% paraformaldehyde in 0.1 M sodium cacodylate buffer, pH 7.4. Kidneys were subsequently dehydrated and embedded in paraffin by standard methods. Four $PKD1^{RC/RC}$ mice at the ages of 25 and 90 days (one of each sex and age) were anaesthetized and injected intravenously through the vena cava with 150 µL 0.1 mg aprotinin (bovine lung aprotinin, SLBW0290, Sigma-Aldrich, St. Louis, MO, USA) diluted in normal saline (Fresenius Kabi, Bad Homburg vor der Höhe, Germany), left for 10 min and perfusion fixed. Kidneys were subsequently paraffin embedded. Aprotinin is an ~6.5-kDa antifibrinolytic molecule and an established high-affinity megalin ligand [14] that is structurally stable, freely filtered in the glomerulus (GL) and endocytosed at the proximal tubular brush border [15]. An overview of the experimental setup is included in Supplementary data, Table S1. Wild-type (WT) mice (C57BL/6) (Taconic Biosciences, Rensselaer, NY, USA) at P25 and P150 days were used as controls to compare antibody specificity.

Cysts counting

Embedded kidneys were cut into 2-µm sections using a microtome (Leica, Wetzlar, Germany). Cysts were defined as structures with a luminal diameter exceeding 50 µm and counted manually. As cysts are not spherical, the diameter was defined as the average of the longest and shortest diameter, measured using cellSens Entry version 2.3 software (Olympus Life Science, Waltham, MA, USA).

Immunoperoxidase (IP) and immunofluorescence (IF) staining and image acquisition

Consecutive cross-sections were cut from the centre of the kidney and placed on SuperfrostPlus object glass slides (Thermo Fisher Scientific, Waltham, MA, USA). The sections were stained as described previously [16] using IP and IF labelling of segment-specific markers: megalin (PT), aquaporin 1 (AQP1; PT, thin descending limb of Henle's loop, vasa recta), sodium–chloride cotransporter (NCC; early distal convoluted tubule), calbindin (late distal convoluted tubule) and aquaporin 2 (AQP2; connecting tubule and collecting duct, collectively referred to as CD). Images were acquired using a motorized, upright widefield slide scanner (Olympus BX61VSU, Olympus Life Science), equipped with an ORCA-Flash 4.0 camera (Hamamatsu Photonics, Hamamatsu City, Japan). Whole slide scans were obtained with a ×40 objective. Image processing and measurements were performed using cellSens Entry version 2.3 software (Olympus Life Science) and basic image acquisition was achieved using OlyVIA version 2.9 software (Olympus Life Science).

IP staining

Primary antibodies Included sheep anti-megalin (1:20 000; gift from Pierre Verroust, France), rabbit anti-AQP1 (1:2000; Merck, Darmstadt, Germany), rabbit anti-NCC (1:000; gift from Mark A. Knepper, USA), mouse anti-calbindin (1:5000; gift from Fitzgerald, UK) and rabbit anti-AQP2 (1:2000; Merck).

Secondary antibodies included polyclonal rabbit anti-sheep immunoglobulin G (IgG; Dako, Glostrup, Denmark), polyclonal goat anti-rabbit IgG (Dako) and polyclonal goat anti-mouse IgG (Dako). All were diluted to a concentration of 1:200. Horseradish peroxidase–conjugated antibodies were activated by incubation with 3,3-diaminobenzidine (PanReac AppliChem ITW Reagents, Chicago, IL, USA) for 10 min. The sections were counterstained with Mayer's haematoxylin (Ampliqon, Odense, Denmark) for 2 min and dehydrated before mounting of coverslips with Eukitt (PanReac AppliChem ITW Reagents).

IF staining

Primary antibodies included sheep anti-megalin (1:10 000; gift from Pierre Verroust, France), rabbit anti-AQP2 (1:1000; Merck) and rabbit anti-aprotinin (1:2000; MyBioSource, San Diego, CA, USA).

Secondary antibodies included Alexa Fluor546 donkey anti-sheep IgG (Invitrogen, Carlsbad, CA, USA) and Alexa Fluor488 donkey anti-rabbit IgG (Invitrogen). All were diluted to a concentration of 1:300. Sections were mounted with coverslips using Fluoroshield mounting medium (Sigma-Aldrich).

Serial sections

From each mouse injected with aprotinin, 200 serial sections were cut from the centre of one kidney. Every second slide was IP labelled with anti-aprotinin (1:2000; MyBioSource) to identify any possible connection between aprotinin-positive cysts and the tubular system and every 10th slide was IF labelled with anti-megalin and anti-AQP2 to establish the tubular expression pattern of the cysts. Cysts were traced through the consecutive sections using OlyVIA version 2.9 software (Olympus Life Science).

Statistical analysis

All quantitative data are presented as mean ± SD. Two-way analysis of variance (ANOVA) was used to compare mean cyst count between the groups (sex and age) and Student's *t*-test was used to assess the differences in mean cyst count between sex within each age group. P-values <0.05 were considered statistically significant.

RESULTS

The number of renal cysts in *PKD1*$^{RC/RC}$ mice increases with age

Renal cysts were observed at all ages and were often located in clusters rather than scattered (Supplementary data, Figure S1). The total number of cysts increased from 22.3 ± 4.54 at P10 to 91.1 ± 15.72 at P180 (Figure 1; Supplementary data, Table S2), showing a statistically significant, positive correlation between the number of cysts and age (P=0.0000001, two-way ANOVA). A trend towards more cysts in male mice was observed (Figure 1), but this was not statistically significant (P=0.8), supporting an age-dependent increase in the number of cysts independent of sex. Five mice at age P90 were excluded due to an extreme outlying phenotype (excessive total kidney volume and number of cysts) when compared with the rest of the animals at the same age (Supplementary data, Table S3). These mice were born following embryo transfer and the phenotype was most likely related to this procedure. Data obtained from these animals is therefore not part of the presented results in the following sections.

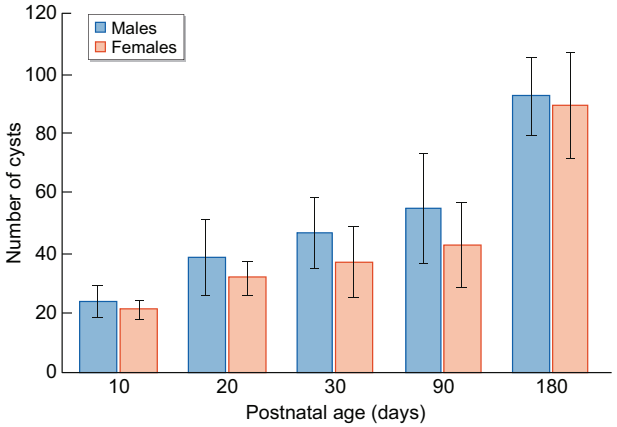

FIGURE 1: Cyst count increases with age. Total cyst count in *PKD1*$^{RC/RC}$ mice at P10, P20, P30, P90 and P180. Data represent the number of cysts per cross-sectional kidney slice and are presented as mean ± SD (data on P90 mice born following embryo transfer are not included). The total number of observed cysts increases as mice age (P = 0.0000001, two-way ANOVA). No significant difference was observed between male and female mice, neither when including all ages (P = 0.8, two-way ANOVA) or when testing each age group (P10: P = 0.4; P20: P = 0.4; P30: P = 0.3; P90: P = 0.6 and P180: P = 0.8, Student's *t*-test). Data from individual mice are summarized in Supplementary data, Table S2.

PKD1$^{RC/RC}$ mice show a switch in tubular marker expression of cysts with age

As cysts develop from different and specific tubular segments, we wanted to describe tubular marker expression in cystic cells, focusing on identifying cysts expressing megalin. As expected, all tubular markers (megalin, AQP1, NCC, calbindin and AQP2) stained the tubule segments in which they are normally expressed (Supplementary data, Figure S2). Expression of all markers, except for NCC, was observed in cysts at all ages. Megalin and AQP1 are co-expressed in the apical membranes of the PT and a similar co-expression was observed in cysts with very few exceptions (data not shown). Also, calbindin and AQP2 are both expressed in connecting tubules, hence most calbindin-positive cysts also expressed AQP2. Kidney sections from all mice were stained with all tubular markers, but in the subsequent data analysis we focused on megalin and AQP2, as they were the most commonly expressed of the analysed membrane proteins in cystic cells and no colocalization of these two markers was observed.

Megalin was expressed in the brush border and endocytic apparatus in cystic cells at all ages (Figure 2A and B). At P10, 56% of the cysts were megalin positive, which decreased to 45% at P20, 25% at P30, 21% at P90 and 16% at P180 (Figure 3). Concomitantly, an increase with age in cysts expressing AQP2 was observed (Figure 3). This switch in tubular marker expression was also noticed when looking at cyst occupancy, with megalin-positive cysts constituting the largest area of the kidney in younger mice and AQP2-positive cyst occupying the largest area in older mice, when comparing the two markers (Figure 4). Interestingly, the fraction of cysts that did not stain for any of the examined tubular markers increased with age (14% at P10 versus 44% at P180) (Figures 3 and 5C). In addition, some of the larger cysts at P20, P30, P90 and P180 seemed to partially lose their expression of megalin, with some parts of the cystic cells being megalin positive, while others appeared negative [Figure 2A (P30 red *) and Figure 5A]. Similar results were observed in cysts expressing AQP2 at P90 and P180 (Figure 5B). Some cystic cells at all ages revealed an altered morphology, with flattened and elongated cells, when compared with the surrounding tubules. The change in cell morphology was independent of megalin and AQP2 expression but was associated with the loss of expression of both markers (Supplementary data, Figure S3).

Megalin mediates endocytosis of aprotinin in cystic cells

To establish if megalin expressed in cystic cells is capable of mediating endocytosis, we injected *PKD1*$^{RC/RC}$ mice at P25 and

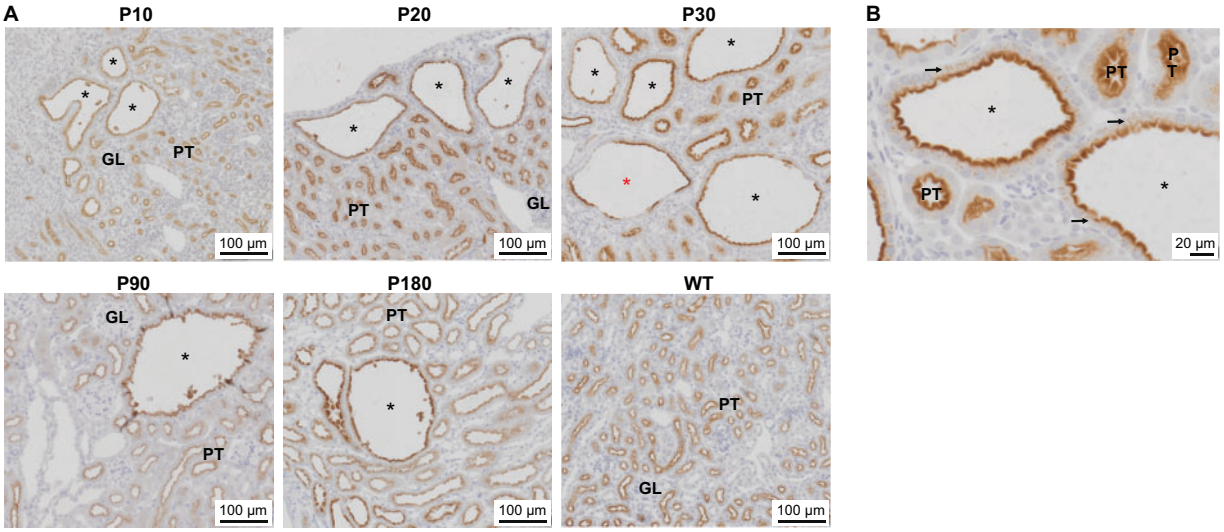

FIGURE 2: Megalin is expressed in cysts at all ages. Representative images showing megalin expression by IP in kidney sections from *PKD1*$^{RC/RC}$ mice at P10, P20, P30, P90 and P180 as well as a WT mouse at P25. (**A**) Megalin is expressed in cysts and PT in all ages. (**B**) Megalin is expressed in the apical brush border and the endocytic apparatus in both cystic cells and PT cells. Scale bar: 100 μm and 20 μm, respectively. Black asterisk: megalin-positive cyst; red asterisk: dedifferentiated cyst; arrows: megalin expression in the endocytic apparatus in cystic cells; PT: proximal tubule; GL: glomerulus.

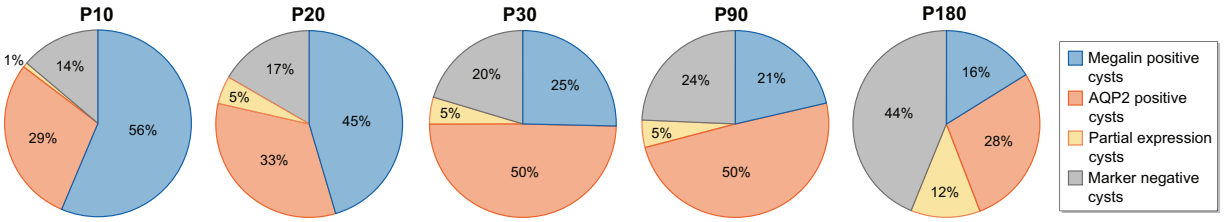

FIGURE 3: Tubular marker expression in cysts changes over time. Pie charts showing the relative proportion of cysts expressing segment-specific tubular markers in *PKD1*$^{RC/RC}$ mice at P10, P20, P30, P90 and P180. Data are presented as means (both male and female mice) for each age group. The relative proportion of megalin-positive cysts decreases with age, whereas the relative proportion of AQP2-positive cysts increases until P90 and then decreases. In addition, the relative proportion of cysts with partial expression or no expression of the examined tubular markers increases with age. Scale bar: 100 μm.

P90 with aprotinin and visualized potential uptake using anti-aprotinin antibody. Aprotinin co-localized with megalin in PTs and cysts. Some megalin-positive cysts with no apparent aprotinin uptake were also observed, demonstrating that the expression of megalin is not sufficient for the uptake into cystic cells (Figure 6A). Diffuse, intracellular positive staining was also observed in some AQP2-positive segments, which may reflect a non-specific mechanism of aprotinin uptake. Megalin-positive cystic cells and PTs revealed granular staining for aprotinin consistent with endocytosis, suggesting that megalin in cystic cells is capable of mediating endocytosis (Figure 6B and C).

Aprotinin uptake into cystic cells depends on a tubule–cyst connection

To determine if a connection between cysts and the tubular system was required for aprotinin uptake, 200 serial sections were prepared from the *PKD1*$^{RC/RC}$ mice injected with aprotinin (Figure 7). All aprotinin-positive cysts were at some point attached to an adjacent tubule segment and aprotinin was absent in megalin-positive cysts with no tubular connection. Hence a persistent connection to the tubular system is necessary for the efficient uptake of injected and filtered aprotinin into megalin-positive cyst lining cells. No significant difference in the proportion of megalin- and aprotinin-positive cysts was observed when comparing mice at P25 [~62% (33–100%)] with mice at P90 [~67% (50–85%)] ($P = 0.79$) (Supplementary data, Table S4).

During the tracing of a mouse at P25, we observed a possible fusion of two separately defined cysts, both attached to the tubular system (Supplementary data, Figure S4A). One part of the cyst showed evidence of aprotinin uptake, whereas the other part was aprotinin negative, suggesting that the cysts may originate from two different tubule segments. Based on morphology and location of a nearby GL, the tubule segment attached to the cyst part positive for aprotinin was most likely a PT segment, whereas the segment without aprotinin uptake could not be identified (Supplementary data, Figure S4B). Sections prior to the tubule–cyst connection were not available and it was therefore not possible to further characterize the tubular marker expression pattern of this tubule segment. Additional immunolabelling showed that the 'fused' cyst was megalin positive, at least in some parts (Supplementary data, Figure S4C).

DISCUSSION

In this hypothesis-generating study, we demonstrate that megalin is expressed in cystic cells and megalin is functional and capable of endocytosing ligands freely filtered in the glomeruli if an intact tubule–cyst connection is present.

The *PKD1*$^{RC/RC}$ mouse model used is characterized by progressive formation of renal cysts over time. The cystic cells selectively express markers specific to various segments of the renal tubular system consistent with previous observations in other ADPKD models [10, 11]. Our observations suggest that

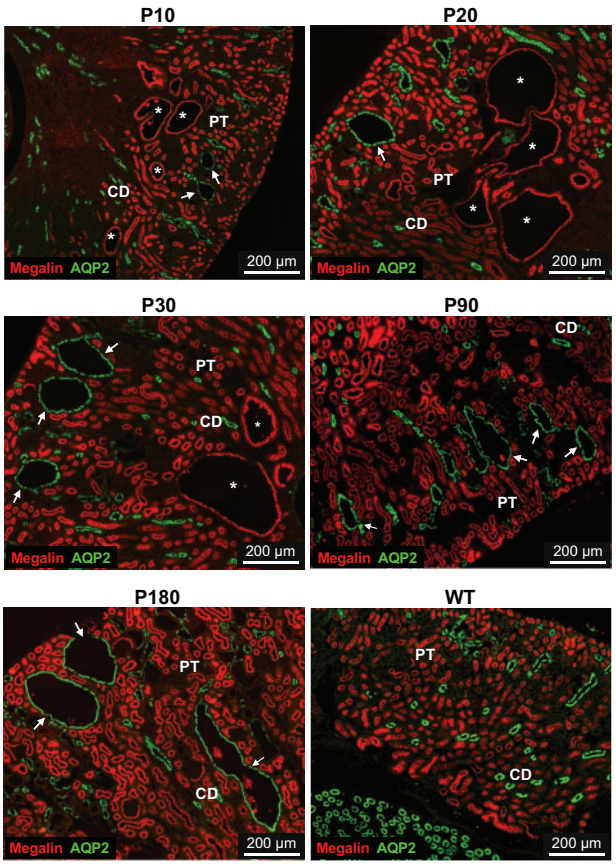

FIGURE 4: Tubular marker expression in cysts changes from megalin to AQP2 over time. Representative images showing expression of megalin (red) and AQP2 (green) by IF labelling in kidney sections from *PKD1*$^{RC/RC}$ mice at P10, P20, P30, P90 and P180 as well as a WT mouse at P25. The dominant tubular marker expression gradually shifts from megalin in early ages to AQP2 in later ages in cysts. Scale bar: 200 μm. Asterisk: megalin-positive cyst; arrow: AQP2-positive cyst; PT: proximal tubule; CD: collecting duct.

cysts originate from both PT and CD segments and a switch in cyst origin occurs, with more cysts being of CD origin with age.

The fractions of cysts with partial or absent expression of any of the examined tubular markers increase with age as disease progresses. This may reflect dedifferentiation of cystic cells characterized by a loss of apical–basal polarity [17], which may also explain the changed morphology of cystic cells, which become flatter and more elongated [18]. Consistent with this, similar results have been observed in other ADPKD mouse models [19]. Thus partial expression of megalin or AQP2 may reflect dedifferentiation that eventually results in loss of expression. Interestingly, the number of cysts originating from PT remains quite stable over time, suggesting dedifferentiation is mainly affecting cysts originating from other tubules. As an alternative to dedifferentiation, the fusion of cysts originating from different tubular segments may lead to partial expression of particular markers. We identified one case of what appears to be two fused cysts clearly attached to different tubular segments. We did not identify any cysts expressing both megalin and AQP2, which may have been expected if cyst fusion was common. Thus it remains unclear if this observation represents a fusion of two cysts or some other process.

Injected aprotinin was internalized by PT cells and megalin-expressing cystic cells, suggesting megalin-mediated endocytosis; however, an intact tubule–cyst connection was required, consistent with the notion that such ligands must be filtered in the GL prior to endocytosis [20]. It is generally accepted that cysts develop from the tubular system and eventually pinch off as they become enlarged [21]. In the *PKD1*$^{RC/RC}$ mouse model, we observed cysts both at P25 and P90 with a diameter $>300\,\mu$m that remained connected to the tubular system. The ratio between cysts positive for both megalin and aprotinin (suggesting an intact tubule–cyst connection) and cysts positive for megalin only (suggesting detachment of cysts from the tubular system) is similar at P25 and P90, implying that the fraction of megalin-positive cysts connected to the tubular system does not decrease with time, at least not until after P90. In humans, the diameter of cysts before detaching has been estimated to 2–3 mm [22], and it has been reported that 20–30% of examined cysts at ESRD remain attached to the tubular system [23].

Megalin-mediated endocytosis has previously been explored experimentally in mice for kidney-specific drug delivery using peptide-based ligands, showing peptides accumulating almost exclusively within the kidneys [13, 24], although megalin is also expressed in other absorptive epithelia [12]. While the above findings may suggest a similar capability of megalin to facilitate uptake of ADPKD-specific agents in renal cysts, our findings

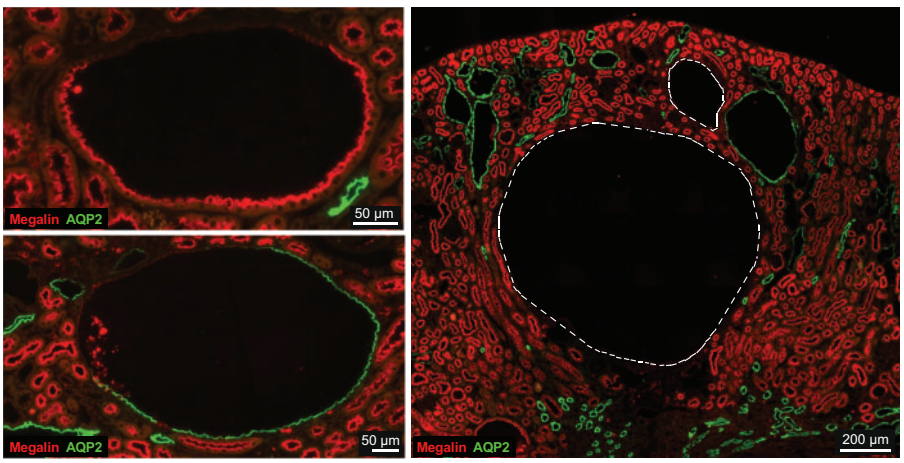

FIGURE 5: Partial and negative marker expression in cysts. Representative images showing megalin (red) and AQP2 (green) expression by IF labelling in kidney sections from a *PKD1*$^{RC/RC}$ mouse at P180. (A) Partial expression of megalinand (B) partial expression of AQP2 in two seperate cysts. (C) Marker-negative cyst indicated bydotted line. Scale bars: 50 μm, 50 μm and 200 μm, respectively.

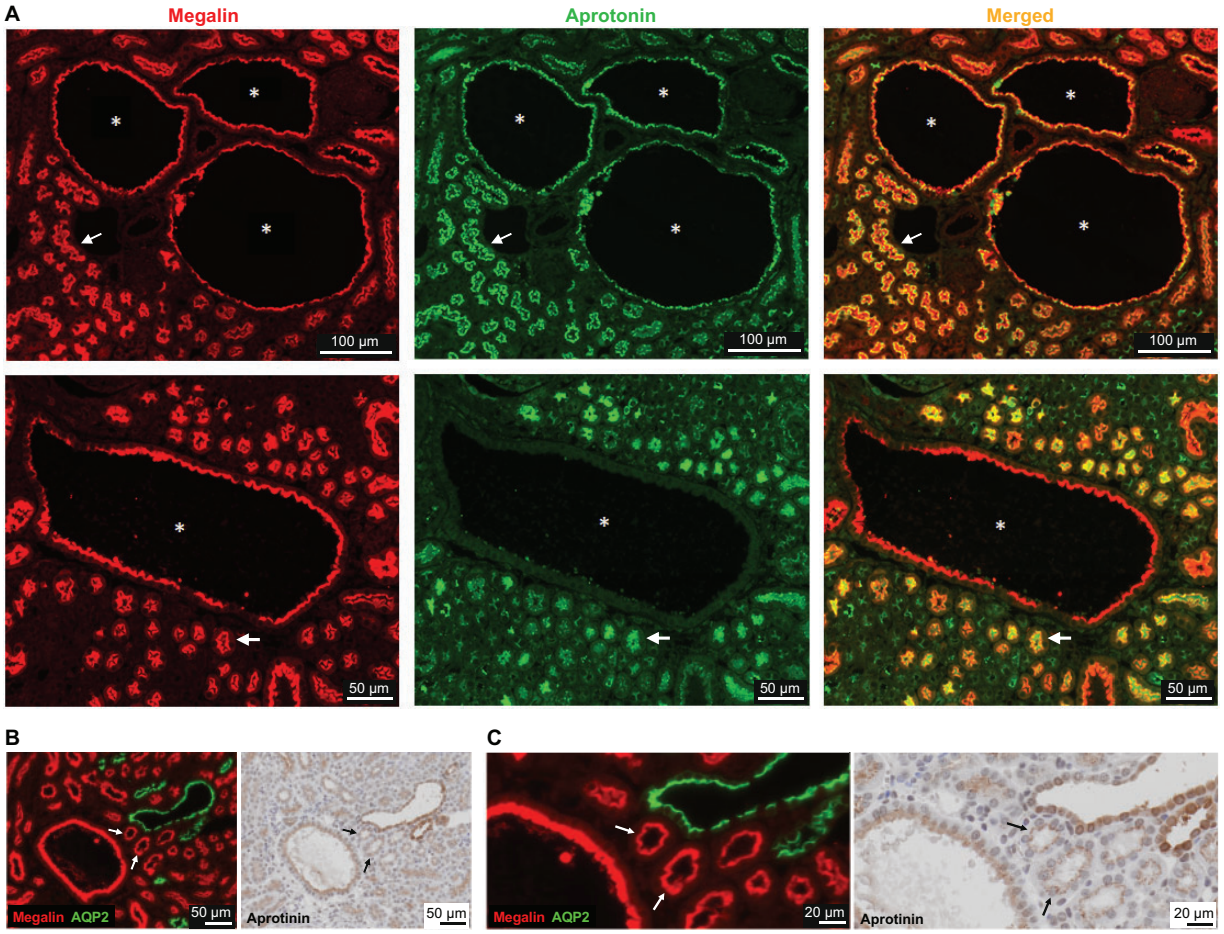

FIGURE 6: Aprotinin is endocytosed into megalin-positive cysts. Representative images showing the expression of megalin and the localization of injected aprotinin by IF and IP labelling in kidney sections from a *PKD1*$^{RC/RC}$ mouse at P25. **(A)** A megalin- (red) and aprotinin-positive (green) cyst (top row), as well as a megalin-positive, but aprotinin-negative cyst (bottom row). Scale bars: 100 μm and 50 μm, respectively. **(B)** Megalin- and AQP2-positive cysts (IF, left) compared with aprotinin staining by IP (right) of an adjacent section. Scale bar: 50 μm. **(C)** Magnification of (B). Scale bar: 20 μm. In the megalin-positive cysts as well as neighbouring PTs, aprotinin labelling is clearly granular and vesicular, reflecting endocytosis, whereas aprotinin labelling of the AQP2-positive cysts is diffuse, possibly reflecting non-specific uptake. Asterisk: megalin-positive cyst; arrow: proximal tubule.

have some important limitations that must be considered. First, manual counting of cysts provides a source of error, as it is a subjective assessment depending on the definition of cysts. We believe that the relatively large number of animals included in the study provides some assurance against random variation and that the relative changes in cyst number and tubular marker expression observed are reliable. Second, all observations are cross-sectional in time, rendering it impossible to make any definite conclusions about the time–space dynamics of cyst formation in the kidney, including cyst origin. However, the use of segment-specific marker expression to characterize cyst origin has been applied in other studies with similar findings [9–11]. Third, the results in rodent models of ADPKD are not always directly transferable to humans [8]. Even though the *PKD1*$^{RC/RC}$ mouse model used in this study is based on a *PKD1* allele (p.R3277C) identified in humans with ADPKD and the model would compare to a consanguineous family with adult-onset ADPKD [9], some differences do exist. In humans, significant gender variability [25, 26], as well as inter- and intrafamilial variability are observed [27], while *PKD1*$^{RC/RC}$ mice of the same age reveal histological phenotypes with very little variation, most likely related to the very homogeneous background genotypes and similar environmental conditions typical to the animal experimental setting. Despite such potential differences, a number of observations in this study are similar to findings in humans, including the increase in cyst number [23, 28] as well as the increase in AQP2-positive or marker-negative cysts with increasing age [23]. In addition, the original article states that reduced renal function was observed in mice from 9 months of age [9], which suggests the observations in this study compare to a time before glomerular filtration rate starts to decline in humans. However, the capability of megalin to facilitate uptake of ADPKD-specific agents in renal cysts was only examined in four mice, hence the results need to be verified in other species, including humans.

In conclusion, in a mouse model of ADPKD, megalin is expressed in renal cysts at ages from P10 to P180, although the proportion of positive cysts decreases with age. The megalin ligand aprotinin is internalized in megalin-positive cystic cells if an open tubule–cyst connection can be preserved. Thus potential treatment approaches using megalin to facilitate uptake of ADPKD-modifying agents probably should be applied in the early stages of the disease and should exert an ADPKD-specific effect that does not affect other megalin-expressing cells and tissues [16].

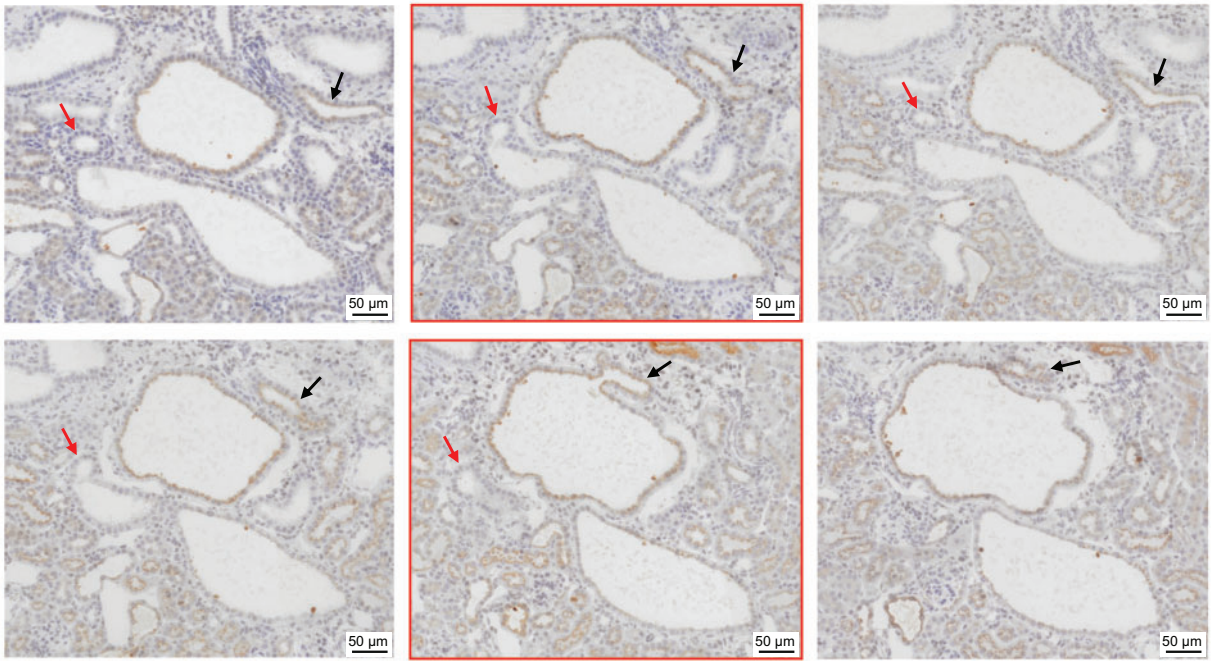

FIGURE 7: Aprotinin-positive and negative cysts are attached to the renal tubular system. Aprotinin uptake was identified by IP staining in kidney serial sections from a *PKD1*$^{RC/RC}$ mouse at P25. The consecutive sections demonstrate the attachment of aprotinin-positive cysts to distinct tubule segments. Red box: sections in which a tubule–cyst connection is evident; black arrow: aprotinin-positive proximal tubule segment; red arrow: aprotinin-negative tubule segment of unknown origin. Scale bar: 50 μm.

SUPPLEMENTARY DATA

Supplementary data are available at ckj online.

ACKNOWLEDGEMENTS

The authors acknowledge the Bioimaging Core Facility, Health, Aarhus University for the use of equipment and support of the imaging facility.
Helle Salling Gittins, Hanne Sidelmann and Inger Blenker Kristoffersen are gratefully acknowledged for their excellent technical assistance.

FUNDING

This work was supported by Vanførefonden, cand. jur. Torkil Steenbeck's Grant, Independent order of Odd Fellows nr. 73 Svend Fælding, Karen Elise Jensen's Fund, O.P. Nielsen, Danish Kidney Association, Danish Society of Nephrology, Fund of 1870 and Central Denmark Region. None of the funders played a role in the collection, analysis or interpretation of data; in the writing of the report; or in the decision to submit the article for publication.

CONFLICT OF INTEREST STATEMENT

M.L.N. reports grants from Vanførefonden, cand. jur. Torkil Steenbeck's Grant, Independent order of Odd Fellows nr. 73 Svend Fælding, Karen Elise Jensen's Fund, Danish Kidney Association, Danish Society of Nephrology, Fund of 1870 and Central Denmark Region during the conduct of the study. V.E.T. reports grants from Otsuka, Palladio, Novartis-Genzyme, Reata, Mironid and Blueprint Medicines and support from Navitor outside the submitted work. P.C.H. reports grants from Otsuka Pharmaceuticals, Navitor and Acceleron and support from Otsuka Pharmaceuticals, Mitobridge, Regulus, Vertex Pharmaceuticals outside the submitted work. H.B. reports grants from Karen Elise Jensen's Fund, Danish Kidney Association, Danish Society of Nephrology, Central Denmark Region and O.P. Nielsen during the conduct of the study. The results presented in this article have not been published previously in whole or part, except in abstract form.

DATA AVAILABILITY STATEMENT

The data underlying this article are available in the article and in its supplementary material.

REFERENCES

1. Lanktree MB, Haghighi A, Guiard E *et al.* Prevalence estimates of polycystic kidney and liver disease by population sequencing. *J Am Soc Nephrol* 2018; 29: 2593–2600
2. Willey CJ, Blais JD, Hall AK *et al.* Prevalence of autosomal dominant polycystic kidney disease in the European Union. *Nephrol Dial Transplant* 2017; 32: 1356–1363
3. The polycystic kidney disease 1 gene encodes a 14 kb transcript and lies within a duplicated region on chromosome 16. The European Polycystic Kidney Disease Consortium. *Cell* 1994; 77: 881–894
4. Mochizuki T, Wu G, Hayashi T *et al.* . *PKD2*, a gene for polycystic kidney disease that encodes an integral membrane protein. *Science* 1996; 272: 1339–1342
5. Cornec-Le Gall E, Alam A, Perrone RD. Autosomal dominant polycystic kidney disease. *Lancet* 2019; 393: 919–935

6. Cornec-Le Gall E, Audrezet MP, Le Meur Y *et al*. Genetics and pathogenesis of autosomal dominant polycystic kidney disease: 20 years on. *Hum Mutat* 2014; 35: 1393–1406
7. Lanktree MB, Chapman AB. New treatment paradigms for ADPKD: moving towards precision medicine. *Nat Rev Nephrol* 2017; 13: 750–768
8. Aguiari G, Catizone L, Del Senno L. Multidrug therapy for polycystic kidney disease: a review and perspective. *Am J Nephrol* 2013; 37: 175–182
9. Hopp K, Ward CJ, Hommerding CJ *et al*. Functional polycystin-1 dosage governs autosomal dominant polycystic kidney disease severity. *J Clin Invest* 2012; 122: 4257–4273
10. Ahrabi AK, Jouret F, Marbaix E *et al*. Glomerular and proximal tubule cysts as early manifestations of *Pkd1* deletion. *Nephrol Dial Transplant* 2010; 25: 1067–1078
11. Walker RV, Keynton JL, Grimes DT *et al*. Ciliary exclusion of Polycystin-2 promotes kidney cystogenesis in an autosomal dominant polycystic kidney disease model. *Nat Commun* 2019; 10: 4072
12. Nielsen R, Christensen EI, Birn H. Megalin and cubilin in proximal tubule protein reabsorption: from experimental models to human disease. *Kidney Int* 2016; 89: 58–67
13. Wischnjow A, Sarko D, Janzer M *et al*. Renal targeting: peptide-based drug delivery to proximal tubule cells. *Bioconjug Chem* 2016; 27: 1050–1057
14. Moestrup SK, Cui S, Vorum H *et al*. Evidence that epithelial glycoprotein 330/megalin mediates uptake of polybasic drugs. *J Clin Invest* 1995; 96: 1404–1413
15. Tenstad O, Williamson HE, Clausen G *et al*. Glomerular filtration and tubular absorption of the basic polypeptide aprotinin. *Acta Physiol Scand* 1994; 152: 33–50
16. Gao S, Hein S, Dagnæs-Hansen F *et al*. Megalin-mediated specific uptake of chitosan/siRNA nanoparticles in mouse kidney proximal tubule epithelial cells enables AQP1 gene silencing. *Theranostics* 2014; 4: 1039–1051
17. Arnaout MA. Molecular genetics and pathogenesis of autosomal dominant polycystic kidney disease. *Annu Rev Med* 2001; 52: 93–123
18. Chang-Panesso M, Humphreys BD. Cellular plasticity in kidney injury and repair. *Nat Rev Nephrol* 2017; 13: 39–46
19. Puri P, Schaefer CM, Bushnell D *et al*. Ectopic phosphorylated Creb marks dedifferentiated proximal tubules in cystic kidney disease. *Am J Pathol* 2018; 188: 84–94
20. Christensen EI, Birn H, Verroust P *et al*. Megalin-mediated endocytosis in renal proximal tubule. *Ren Fail* 1998; 20: 191–199
21. Paul BM, Vanden Heuvel GB. Kidney: polycystic kidney disease. *Wiley Interdiscip Rev Dev Biol* 2014; 3: 465–487
22. Grantham JJ, Cook LT, Wetzel LH *et al*. Evidence of extraordinary growth in the progressive enlargement of renal cysts. *Clin J Am Soc Nephrol* 2010; 5: 889–896
23. Grantham JJ, Geiser JL, Evan AP. Cyst formation and growth in autosomal dominant polycystic kidney disease. *Kidney Int* 1987; 31: 1145–1152
24. Lenhard SC, McAlexander A, Virtue A *et al*. In vivo imaging of small molecular weight peptides for targeted renal drug delivery: a study in normal and polycystic kidney diseased mice. *J Pharmacol Exp Ther* 2019; 370: 786–795
25. Harris PC, Bae KT, Rossetti S, *et al*. Cyst number but not the rate of cystic growth is associated with the mutated gene in autosomal dominant polycystic kidney disease. *J Am Soc Nephrol* 2006; 17: 3013–3019
26. Johnson AM, Gabow PA. Identification of patients with autosomal dominant polycystic kidney disease at highest risk for end-stage renal disease. *J Am Soc Nephrol* 1997; 8: 1560–1567
27. Torres VE, Harris PC, Pirson Y. Autosomal dominant polycystic kidney disease. *Lancet* 2007; 369: 1287–1301
28. Bae KT, Zhou W, Shen C *et al*. Growth pattern of kidney cyst number and volume in autosomal dominant polycystic kidney disease. *Clin J Am Soc Nephrol* 2019; 14: 823–833